# Effect of host paramagnetic ions on the $Gd^{3+}$ EPR linewidth in diluted Van-Vleck paramagnets $Tm_xLu_{1-x}PO_4$ and $Ho_xY_{1-x}VO_4$ and EPR spectra of $Er^{3+}$ in $Ho_xY_{1-x}VO_4$

Sushil K. Misra and Serguei I. Andronenko*
*Department of Physics, Concordia University, 1455 de Maisonneuve Boulevard West, Montreal, Quebec, Canada H3G 1M8*
(Received 10 November 1995; revised manuscript received 10 January 1996)

$Gd^{3+}$ EPR linewidths in diluted Van-Vleck paramagnets $Ho_xY_{1-x}VO_4$ ($x=0.0$, 0.02, 0.05, 0.1, 0.15, 0.25, 0.3, 0.5, 0.9, 1.0) and $Tm_xLu_{1-x}PO_4$ ($x=0.0$, 0.1, 0.2, 0.4, 0.6, 0.8, 1.0) were measured at *X* band (8.7–9.6 GHz) in the temperature range 4.2–300 K as functions of temperature and concentration ($x$) of the host paramagnetic ions, $Ho^{3+}$ and $Tm^{3+}$, respectively. It was found that the dipole-dipole and exchange interactions significantly influenced the measured linewidths in $Ho_xY_{1-x}VO_4$ and $Tm_xLu_{1-x}PO_4$ samples for the concentrations $x>0.1$ and $x>0.6$, respectively. Further, in $Ho_xY_{1-x}VO_4$ samples with $x>0.3$ the EPR lines disappeared at temperatures above 10 K due to the formation of percolation clusters by $Ho^{3+}$ ions; the disorder was deduced to have a negligible effect in these hosts. Interaction of the lattice with the electronic quadrupole moment of $Ho^{3+}$ ions created different structural sites of $Gd^{3+}$ in $Ho_xY_{1-x}VO_4$ samples with $x>0.1$ depending on the number of $Ho^{3+}$ ions in the immediate neighborhood of a $Gd^{3+}$ ion, resulting in the observation of up to three different sets of $Gd^{3+}$ EPR spectra. As for $Tm_xLu_{1-x}PO_4$ samples with $0.1<x<0.8$, it was the disorder, rather than a percolation cluster, that dominated the $Gd^{3+}$ EPR linewidths due to the rather large difference in the ionic radii of $Tm^{3+}$ and $Lu^{3+}$ ions, as well as in the unit-cell parameters of $TmPO_4$ and $LuPO_4$. The temperature variation of the linewidths were found to be in accordance with those of the average magnetic moments of $Ho^{3+}$ and $Tm^{3+}$ ions in $Ho_xY_{1-x}VO_4$ and $Tm_xLu_{1x}PO_4$, respectively. $Gd^{3+}$ spin-Hamiltonian parameters were estimated at different temperatures for the two families of hosts. EPR spectra of the $Er^{3+}$ ion, present as a chemical impurity, have also been observed in $Ho_xY_{1-x}VO_4$ samples at liquid-helium temperatures.

## I. INTRODUCTION

$TmPO_4$, $LuPO_4$ and $HoVO_4$, $YVO_4$ belong to the series of lanthanide phosphates and vanadates, respectively, possessing the tetragonal zircon structure characterized by the space group $D_{4h}^{19}$. These compounds have been of interest recently, because of (i) $TmPO_4$ exhibiting cooperative Jahn-Teller effect, leading to the softening of the elastic constant at about 20 K,[1] thus lowering the symmetry under the action of a high magnetic field[2] due to magnetoelastic interactions; (ii) ordering of Ho and Tm nuclear magnetic moments at very low temperatures,[3,4] (iii) suitability of $HoVO_4$ for enhanced nuclear cooling,[5] and (iv) usefulness (e.g., $LuPO_4$) for confinement of radioactive nuclear wastes.[6]

EPR investigations of $Gd^{3+}$ in the pure diamagnetic lattices of $LuPO_4$ and $YVO_4$ have been reported by Rappaz, Boatner, and Abraham[6] and by Rosenthal,[7] respectively. As for the pure paramagnetic lattices, strong influence of dynamical exchange and dipole interactions on EPR linewidth of $Gd^{3+}$ was reported by Mehran and co-workers[8,9] in $TmPO_4$. In addition, Mehran, Stevens, and Plaskett deduced inhomogeneous broadening of EPR lines by indirect superhyperfine interaction between $Gd^{3+}$ ion and $^{165}Ho$ nuclei in $HoVO_4$,[10] and the influence of Jahn-Teller-induced random strains on the $Gd^{3+}$ EPR spectra in mixed crystals $Tm_xY_{1-x}VO_4$.[11] Dilution of $Gd^{3+}$-doped paramagnetic lattices of $TmPO_4$ and $HoVO_4$ by the diamagnetic ions $Lu^{3+}$ and $Y^{3+}$, respectively, reduces the number of paramagnetic ions in the neighborhood of the impurity ion ($Gd^{3+}$), decreasing the influence of interactions between $Gd^{3+}$ and the paramagnetic host ions. Accordingly, a systematic study of magnetically diluted samples $Ho_xY_{1-x}VO_4$ and $Tm_xLu_{1-x}PO_4$, with different concentrations $x$ can be used to understand the behavior of EPR linewidths of the impurity ion $Gd^{3+}$ in these compounds, influenced significantly by exchange and dipole-dipole interactions with the host paramagnetic ions $Ho^{3+}$ or $Tm^{3+}$, interactions with electric crystalline field, and electron-phonon interactions.[8–13]

An optical study of the mixed rare-earth crystals, such as $Y_xLu_{1-x}F_3$, $Yb_xY_{1-x}F_3$, $Yb_xGd_{1-x}F_3$, revealed the importance of disorder as deduced from spectral linewidths of the impurity ion $Er^{3+}$.[14] Theoretical studies on EPR linewidth behavior in mixed magnetically dilute rare-earth crystals have been reported recently by Misiak, Misra, and Mikolajczak,[15] and by Misiak, Misra, and Orhun[16] on $LiYb_xY_{1-x}F_x$ single crystals, and by Misra and Orhun[17] on $Pr_xLa_{1-x}F_3$ single crystals. Percolation-cluster model was applied by Misra and Orhun[18] to explain the behavior of $Gd^{3+}$ EPR linewidths in $LiYb_xY_{1-x}F_4$, according to which, a percolation cluster extends across the sample broadening the EPR lines sharply as a result of shortened spin-lattice relaxation times when the concentration of the paramagnetic ions exceeds a certain critical value.

The purpose of this paper is to present detailed systematic experimental data on $Gd^{3+}$ EPR spectra in diluted paramagnetic $Ho_xY_{1-x}VO_4$ and $Tm_xLu_{1-x}PO_4$ crystals as function of concentration ($x$) of the host paramagnetic ions at different temperatures in the range 4.2–300 K. The EPR linewidth data will be analyzed in order to (i) understand the interactions between the impurity $Gd^{3+}$ ion and the host paramag-

 

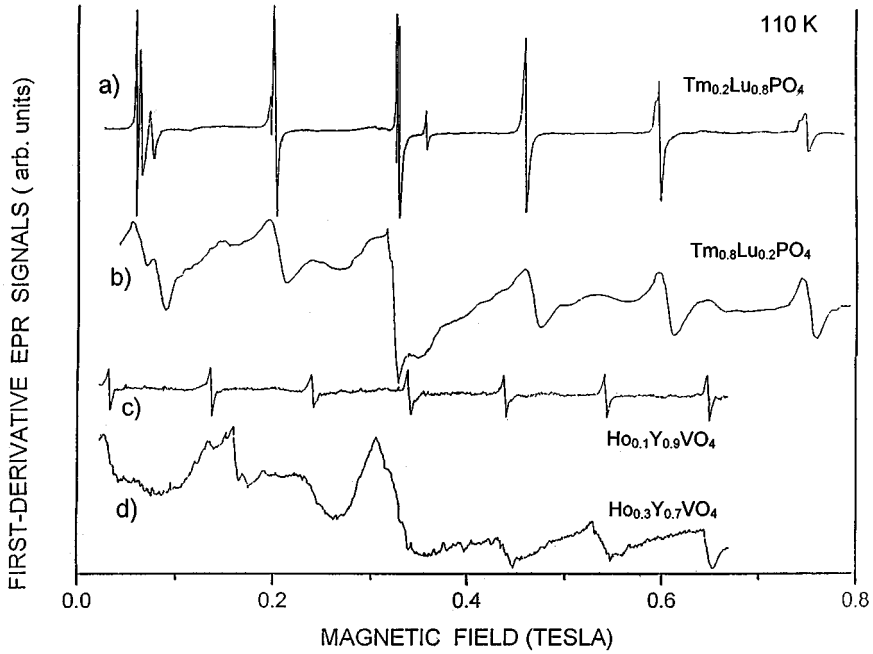


FIG. 1. Typical $X$-band (9.6 GHz) $Gd^{3+}$ EPR spectra in $Tm_xLu_{1-x}PO_4$ and $Ho_xY_{1-x}VO_4$ for $\mathbf{B}\|Z$ axis at 100 K: (a) $Tm_{0.2}Lu_{0.8}PO_4$, (b) $Tm_{0.8}Lu_{0.2}PO_4$, (c) $Ho_{0.1}Y_{0.9}VO_4$, (d)$Ho_{0.3}Y_{0.7}VO_4$.

netic ions in $Ho_xY_{1-x}VO_4$ and $Tm_xLu_{1-x}PO_4$ crystals; (ii) discern the mechanisms that influence $Gd^{3+}$ EPR linewidth in these two families of crystals; and (iii) estimate $Gd^{3+}$ spin-Hamiltonian parameters in these hosts. In addition, an effort will be made to assess the extent to which (i) the crystal structures become distorted as functions of $x$; and (ii) the two rare-earth ions $Ho^{3+}$ and $Tm^{3+}$ are magnetically similar. The presence of $Er^{3+}$ ions as a chemical impurity has provided an opportunity to study $Er^{3+}$ spectra in $Ho_xY_{1-x}VO_4$, as presented in Sec. VI.

## II. PREPARATION OF SAMPLES

$Tm_xLu_{1-x}PO_4$ ($x=0.0$, 0.1, 0.2, 0.4, 0.6, 0.8, 1.0) single crystals characterized by tetragonal structure were prepared in the form of parallelepipeds with well-developed (100), (010), (001) faces by the flux-growth technique described by Smith and Wanklin[19] $Ho_xY_{1-x}VO_4$ ($x=0.0$, 0.02, 0.05, 0.1, 0.15, 0.25, 0.3, 0.5, 0.8, 0.9, 1.0) single crystals with well-defined (100), (010), (001) faces whose largest dimension was along the $c$ axis were grown using Czochralsky's technique.[20] The impurity content of $Gd^{3+}$ in both these series of crystals was about 0.2%. They were grown at the Institute of Silicate Chemistry, Russian Academy of Sciences, St. Petersburg.

## III. EPR DATA

EPR spectra were recorded on a Bruker (ER 200D) spectrometer (100-kHz modulation) in the temperature range 77–300 K, and on a Varian $X$ band V-4502 spectrometer in the temperature range 4.5–110 K (400-Hz modulation). The temperature was varied using a heater resistor inside a commercial liquid-helium cryostat by the use of a homemade cavity for measurements at temperatures below 110 K.

EPR spectra were recorded at different temperatures in $Tm_xLu_{1-x}PO_4$ and $Ho_xY_{1-x}VO_4$ samples to deduce temperature dependences of $Gd^{3+}$ EPR linewidths of the allowed transitions $M\leftrightarrow M-1$($M=7/2$, 5/2, 3/2, 1/2, $-1/2$, $-3/2$, $-5/2$, $-7/2$, is the electronic magnetic quantum number of the $Gd^{3+}$ ion, characterized by the electronic spin $S=7/2$) for the orientation of the external magnetic field ($\mathbf{B}$) parallel to the magnetic $Z$ axis. (The magnetic $Z$, $X$, and $Y$ axes are defined to be those directions of $\mathbf{B}$ for which extrema of fine-structure splittings occur; these splittings are in decreasing order, respectively, for $\mathbf{B}\|Z,X,Y$ and were found to be coincident with the crystallographic axes $c$, $a$, and $b$, respectively.) More details on $Gd^{3+}$ EPR spectra in $TmPO_4$ and $HoVO_4$ are described in Refs. 6–13.

In particular, typical $Gd^{3+}$ spectra as recorded for $\mathbf{B}\|Z$ axis in $Tm_{0.2}Lu_{0.8}PO_4$, $Tm_{0.8}Lu_{0.2}PO_4$, $Ho_{0.1}Y_{0.9}VO_4$, $Ho_{0.3}Y_{0.7}VO_4$ at 110 K are exhibited in Fig. 1. It is seen that in $Tm_{0.2}Lu_{0.8}PO_4$ sample, in addition to the seven intense allowed fine-structure lines, there appeared another overlapping set of $Gd^{3+}$ lines. This is due to creation of magnetically inequivalent sites by disorder in the crystal as explained in Sec. V. In Fig. 2 are exhibited $Gd^{3+}$ spectra in $Tm_{0.8}Lu_{0.2}PO_4$ and $Ho_{0.3}Y_{0.7}VO_4$ samples as observed at 5 K. The three sets of observed $Gd^{3+}$ EPR lines in $Ho_{0.3}Y_{0.7}VO_4$ at 5 K appear due the presence of three magnetically inequivalent $Gd^{3+}$ sites created by the interaction of the electronic quadrupole moments of $Ho^{3+}$ ions with the lattice of $HoVO_4$.[21] (More details in Sec. V.) The line at $g_\parallel=3.559$ observed in the EPR spectra of $Ho_{0.3}Y_{0.7}VO_4$ at 5 K (Fig. 2) is identified as the EPR line due to the $Er^{3+}$ ions present as an impurity, because its $g$ value ($g_\parallel=3.544$) is the same as that for $Er^{3+}$ in $YVO_4$ reported by Ranon.[22] The shape of all the EPR lines was found to be Lorentzian. The intensity of the EPR lines decreased with increasing con-

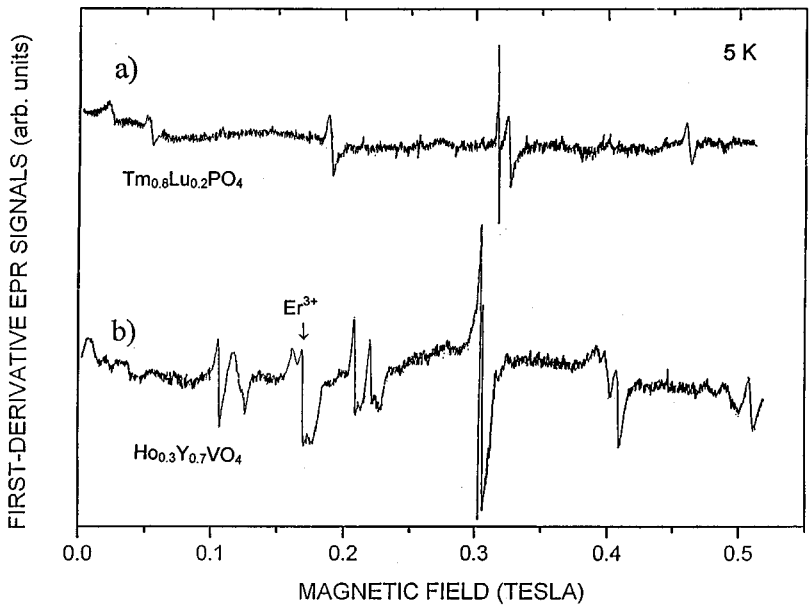


FIG. 2. Typical *X*-band (8.7–8.9 GHz) $Gd^{3+}$ EPR spectra in $Tm_xLu_{1-x}PO_4$ and $Ho_xY_{1-x}VO_4$ for $\mathbf{B}\|Z$ axis at 5 K: (a) $Tm_{0.8}Lu_{0.2}PO_4$, (b) $Ho_{0.3}Y_{0.7}VO_4$. (The $Er^{3+}$ EPR line has also been indicated.)

centration ($x$) of the host paramagnetic ions for both $Ho_xY_{1-x}VO_4$ and $Tm_xLu_{1-x}PO_4$ samples at any temperature.

## IV. SPIN-HAMILTONIAN PARAMETERS

The EPR line positions of the $Gd^{3+}$ ion, substituting for the rare-earth $Lu^{3+}$, $Y^{3+}$, $Tm^{3+}$ or $Ho^{3+}$ ions in $Tm_xLu_{1-x}PO_4$ and $Ho_xY_{1-x}VO_4$, characterized by $D_{2d}$ point-group symmetry at their sites,[23] were fitted to the following spin-Hamiltonian, appropriate to tetragonal site symmetry:

$$H=\mu_B[g_\perp(B_xS_x+B_yS_y)+g_\|BS_z]+\frac{1}{3}b_2^0O_2^0 + \frac{1}{60}(b_4^0O_4^0+b_4^4O_4^4)+\frac{1}{1260}(b_6^0O_6^0+b_6^4O_6^4). \quad (1)$$

In Eq. (1), the first term describes the Zeeman interaction of the $Gd^{3+}$ ion with the external magnetic field, while the remaining terms describe the interaction between the $Gd^{3+}$ ion and the crystalline electric field (CEF). The $O_n^m$ are spin operators, as defined by Abragam and Bleaney.[24] All the EPR line positions recorded for several orientations of **B** were used in a simultaneous fitting to estimate spin-Hamiltonian parameters by the least-squares technique as described by Misra.[25] In the 80–300 K temperature range, the estimated $g$ values were found to be practically independent of temperature: $g_\perp=g_\|=1.992\pm0.002$ for all the investigated $Ho_xY_{1-x}VO_4$ and $Tm_xLu_{1-x}PO_4$ samples. The zero-field splitting parameters $b_2^0$ for both $Tm_xLu_{1-x}PO_4$ and $Ho_xY_{1-x}VO_4$, for all values of $x$, were found to be linearly dependent on temperature ($T$) in the range 80–300 K. For $Tm_xLu_{1-x}PO_4$ (GHz): $b_2^0=-1.976+2.08\times10^{-4}$ T and for $Ho_xY_{1-x}VO_4$(GHz): $b_2^0=-1.474+5.19\times10^{-4}$ T for all concentrations within experimental error ($\pm0.015$ GHz). These values are in accordance with those reported for the pure lattices of $TmPO_4$ (Ref. 8) and $YVO_4$.[26] The remaining parameters have much smaller values relative to $b_2^0$, and were estimated to have about the same values as those reported in Refs. 6 and 7 for $Gd^{3+}$ in $LuPO_4$ and $YVO_4$, respectively. Specially, for $Ho_xY_{1-x}VO_4$: $b_4^0=-0.0045$ GHz, $b_4^4=0.125$ GHz, $b_6^0=0.0015$ GHz, $b_6^4=0.00015$ GHz, and for $Tm_xLu_{1-x}PO_4$: $b_4^0=-0.015$ GHz, $b_4^4=0.06$ GHz, $b_6^0=0.003$ GHz, $b_6^4=0.004$ GHz. In the liquid-helium temperature range (4.5–10 K) for $Gd^{3+}$ in $Tm_{0.8}Lu_{0.2}PO_4$: $b_2^0=-1.960\pm0.005$ GHz, $g_\|=1.985\pm0.005$, while the values of the parameter $b_2^0$ corresponding to the three well-resolved $Gd^{3+}$ EPR spectra in $Ho_{0.3}Y_{0.7}VO_4$ were estimated to be $-1.387\pm0.005$ GHz, $-1.280\pm0.005$ GHz, and $-1.160\pm0.005$ GHz, the $g$ values being the same for these three sets: $g_\|=1.980\pm0.002$. At 5 K in $Ho_{0.25}Y_{0.75}VO_4$, $Ho_{0.15}Y_{0.85}VO_4$, $Ho_{0.1}Y_{0.9}VO_4$, and $Ho_{0.05}Y_{0.95}VO_4$ samples the same values of the parameters were found: $b_2^0=-1.425\pm0.005$ and $g_\|=-1.982\pm0.002$. In $Ho_{0.25}Y_{0.75}VO_4$ and $Ho_{0.15}Y_{0.85}VO_4$ the values of the parameter $b_2^0$ corresponding to the second less intense $Gd^{3+}$ EPR spectrum were estimated to be the same: $b_2^0=-1.285\pm0.005$ GHz. (At liquid-helium temperature the value of $g_\perp$ could not be determined as EPR spectra for $\mathbf{B}\perp Z$ axis could not be observed for both $Tm_xLu_{1-x}PO_4$ and $Ho_xY_{1-x}VO_4$ samples.)

*$Er^{3+}$ ion.* The $g_\|$ values for the $Er^{3+}$ ion ($S=1/2$) at 5 K were estimated to be $3.559\pm0.005$, $3.585\pm0.005$, $3.585\pm0.005$, $3.590\pm0.005$, and $3.582\pm0.005$ for $Ho_{0.3}Y_{0.7}VO_4$, $Ho_{0.25}Y_{0.75}VO_4$, $Ho_{0.15}Y_{0.85}VO_4$, $Ho_{0.1}Y_{0.9}VO_4$, and $Ho_{0.05}Y_{0.95}VO_4$, respectively. The broad EPR lines, with the linewidths 270 and 280 G characterized by the same values of $g_\|=3.700\pm0.005$ observed in $Ho_{0.9}Y_{0.1}VO_4$ and $HoVO_4$ samples, respectively, in the temperature range 4–10 K, were also identified to be that due to the $Er^{3+}$ ion.

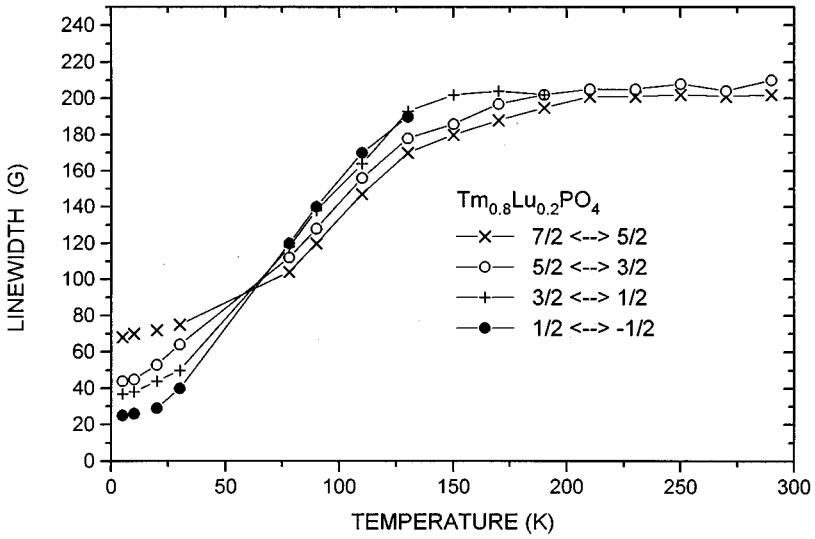


FIG. 3. Temperature dependence of $Gd^{3+}$ EPR linewidths (G=Gauss$=10^{-4}$ T) in $Tm_{0.8}Lu_{0.2}PO_4$ for $\mathbf{B}\|Z$ axis. Widths of unresolved lines (at some temperatures) are not indicated. It is noted that the widths of the EPR lines for the transitions $M\leftrightarrow M-1$ and $-M\leftrightarrow-(M-1)$ are the same.

## V. EPR LINEWIDTHS

In general, the linewidths depended on temperature and concentration ($x$) of the host ions. The temperature dependences of the $Gd^{3+}$ EPR linewidths for $\mathbf{B}\|Z$ axis in $Tm_{0.8}Lu_{0.2}PO_4$ and $Ho_xY_{1-x}VO_4$ ($x=0.1$, 0.15, 0.25, 0.3) samples are shown in Figs. 3 and 4, respectively. The widths of the lines corresponding to the transitions $M\leftrightarrow M-1$ and $-M\leftrightarrow-(M-1)$ were found to be the same within experimental error for all samples.

$Gd^{3+}$ EPR linewidths in $Tm_xLu_{1-x}PO_4$ and $Ho_xY_{1-x}VO_4$ samples do not change significantly with temperature for samples with $x=0.0$, 0.1, 0.2, 0.4, 0.6, and with $x=0.00$, 0.02, and 0.05, respectively. They are thus listed only at 78 and 300 K in Tables I and II, respectively. Generally, $Gd^{3+}$ EPR linewidths for the orientation of **B** parallel to the $X$ and $Y$ axes were found to be the same as those for the orientation of **B** parallel to the $Z$ axis for both $Tm_xLu_{1-x}PO_4$ and $Ho_xY_{1-x}VO_4$. However, in $Ho_xY_{1-x}VO_4$ samples, especially below 110 K, the linewidths for $\mathbf{B}\|X$, $Y$ axes are larger than those observed for $\mathbf{B}\|Z$ axis. The linewidths as functions of the concentration ($x$) of the paramagnetic ions for the samples $Tm_xLu_{1-x}PO_4$ at 77 K, and for the samples $Ho_xY_{1-x}VO_4$ at 110 and 5 K, are shown in Figs. 5, 6, and 7, respectively.

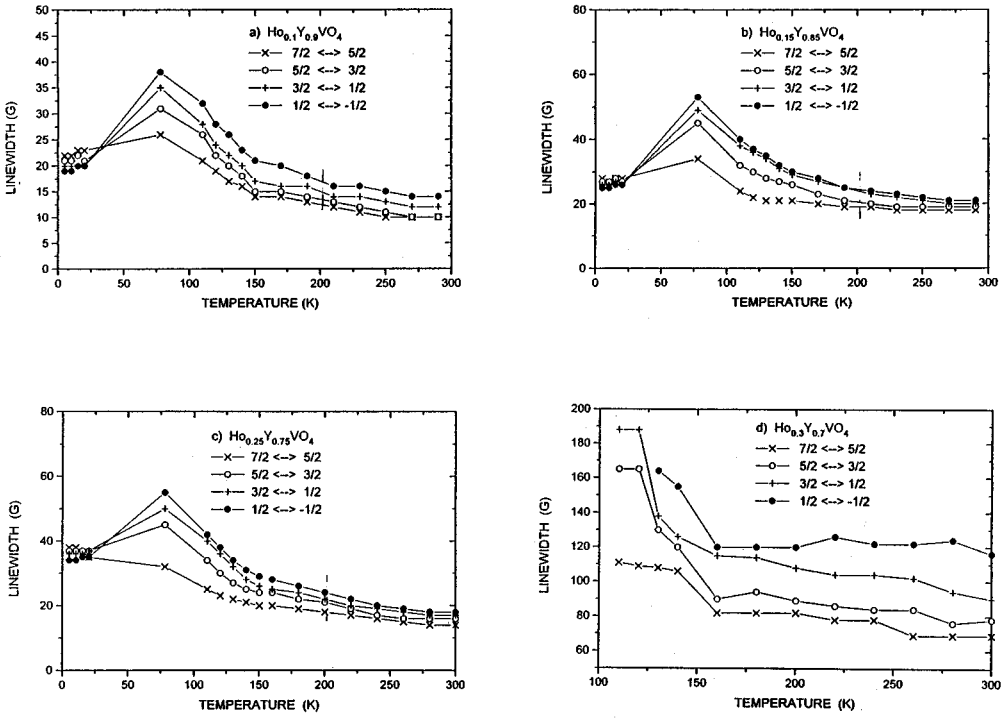


FIG. 4. Temperature dependence of $Gd^{3+}$ EPR linewidths (G=Gauss$=10^{-4}$ T) in $Ho_xY_{1-x}VO_4$ for $\mathbf{B}\|Z$ axis. Widths of unresolved lines (at some temperatures) are not indicated: (a) $x=0.1$, (b) $x=0.15$, (c) $x=0.25$, (d) $x=0.3$. The widths of the EPR lines for the transitions $M\leftrightarrow M-1$ and $-M\leftrightarrow-(M-1)$ are the same. For $Ho_{0.3}Y_{0.7}VO_4$ $Gd^{3+}$ EPR linewidths at 4–10 K are not shown, as they have already been mentioned in Sec. V.

TABLE I. $Gd^{3+}$ EPR linewidths in $Tm_xLu_{1-x}PO_4$ samples as observed for the external magnetic-field orientation along the magnetic $Z$ axis at 78 and 290 K. Here $\Delta B_1$, $\Delta B_2$, $\Delta B_3$, $\Delta B_4$ represent, respectively, the widths of the lines corresponding to the transitions $\pm 7/2 \leftrightarrow \pm 5/2$, $\pm 5/2 \leftrightarrow \pm 3/2$, $\pm 3/2 \leftrightarrow \pm 1/2$, $-1/2 \leftrightarrow +1/2$. The average experimental errors are $\pm 1$ G for $x=0.1$ and 0.2, $\pm 5$ for $x=0.4$ and $\pm 7$ G for $x=0.6$. It is noted that for the sample with $x=0.6$, the EPR lines are observed only below about 140 K.

| Concentration ($x$) | Temperature (K) | $\Delta B_1$ (G) | $\Delta B_2$ (G) | $\Delta B_3$ (G) | $\Delta B_4$ (G) |
|---|---|---|---|---|---|
| 0.0 | 78 | 4.5 | 4.0 | 3.7 | 3.5 |
| | 290 | 4.5 | 4.0 | 3.7 | 3.5 |
| 0.1 | 78 | 32 | 24 | 16 | 8 |
| | 290 | 36 | 22 | 16 | 8 |
| 0.2 | 78 | 41 | 30 | 20 | 16 |
| | 290 | 42 | 34 | 24 | 16 |
| 0.4 | 78 | 133 | 87 | 76 | 72 |
| | 290 | 139 | 90 | 81 | 76 |
| 0.6 | 5 | | 70 | 55 | 40 |
| | 78 | 156 | 125 | 114 | 87 |
| | 140 | 183 | 147 | 122 | 91 |

### Lifetime broadening

For a $Tm_{0.8}Lu_{0.2}PO_4$ sample (Fig. 3), and for $Ho_xY_{1-x}VO_4$ samples with $x=0.1$, 0.15, 0.25, and 0.3 (Fig. 4), it is found that the central line corresponding to the fine-structure transition $-1/2 \leftrightarrow 1/2$ is the broadest, while the outer lines corresponding to the fine-structure transitions $\pm 3/2 \leftrightarrow \pm 1/2$, $\pm 5/2 \leftrightarrow \pm 3/2$, $\pm 7/2 \leftrightarrow \pm 5/2$, become successively narrower. One such behavior was explained satisfactorily by Mehran and Stevens[12] by invoking ''lifetime broadening,'' which takes into account magnetic dipole and exchange interactions between the impurity ion $Gd^{3+}$ and the host paramagnetic ions, explained as follows.

The magnetic moments of the host paramagnetic ions subjected to lattice vibrations produce fluctuating dipolar and exchange fields $B_1^1$ at the $Gd^{3+}$ sites, which induce $\Delta M = \pm 1$ transitions within the energy levels of the $Gd^{3+}$ ion. This results in ''lifetime broadening'' of the energy level $M$ of $Gd^{3+}$, given by the following expression:[12]

TABLE II. $Gd^{3+}$ EPR linewidths in $Ho_xY_{1-x}VO_4$ for the external magnetic-field orientation along the magnetic $Z$ axis at 78 and 300 K. Here $\Delta B_1$, $\Delta B_2$, $\Delta B_3$, $\Delta B_4$ represent, respectively, the widths of the EPR lines corresponding to the transitions $\pm 7/2 \leftrightarrow \pm 5/2$, $\pm 5/2 \leftrightarrow \pm 3/2$, $\pm 3/2 \leftrightarrow \pm 1/2$, $-1/2 \leftrightarrow +1/2$. The averaged experimental error is $\pm 0.5$ G.

| Concentration ($x$) | Temperature (K) | $\Delta B_1$ (G) | $\Delta B_2$ (G) | $\Delta B_3$ (G) | $\Delta B_4$ (G) |
|---|---|---|---|---|---|
| 0.0 | 78 | 4.5 | 4.2 | 3.8 | 3.5 |
| | 300 | 4.5 | 4.2 | 3.8 | 3.5 |
| 0.02 | 78 | 7.1 | 5.5 | 4.7 | 3.5 |
| | 300 | 7.1 | 5.5 | 4.7 | 3.5 |
| 0.05 | 78 | 10.5 | 10.5 | 10.5 | 10.5 |
| | 300 | 14.5 | 13.5 | 12.5 | 10.5 |

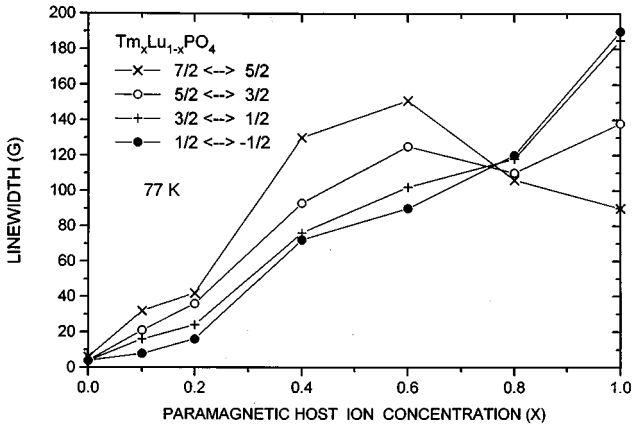


FIG. 5. Dependence of $Gd^{3+}$ EPR linewidths (G=Gauss $=10^{-4}$ T) in $Tm_xLu_{1-x}PO_4$ on concentration ($x$) of the host paramagnetic ions $Tm^{3+}$ for $\mathbf{B} \| Z$ axis at 77 K. The widths of the EPR lines corresponding to the transitions $M \leftrightarrow M-1$ and $-M \leftrightarrow -(M-1)$ are the same.

$$\Delta B(M) = \Delta B_+ + \Delta B_- = a[|\langle M+1|S_+|M\rangle|^2 + |\langle M-1|S_-|M\rangle|^2] \quad (2)$$

The ''lifetime broadening'' for the energy level characterized by the quantum number $M$ arises due to the transitions to the levels $M \pm 1$. Since the transition probabilities are proportional to $|\langle M \pm 1|S_\pm|M\rangle|^2$, the resulting width of the EPR resonance line corresponding to the transition $M \leftrightarrow M-1$ can be expressed as

$$\Delta B(M \leftrightarrow M-1) = \Delta B(M) + \Delta B(M-1) = b[2S(S+1) - 2M(M-1) - 1]. \quad (3)$$

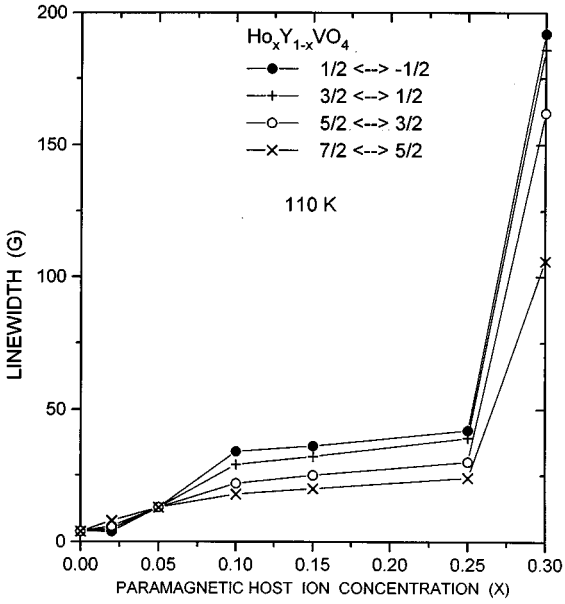


FIG. 6. Dependence of $Gd^{3+}$ EPR linewidths (G=Gauss $=10^{-4}$ T) in $Ho_xY_{1-x}VO_4$ on concentration ($x$) of the host paramagnetic ions $Ho^{3+}$ for $\mathbf{B} \| Z$ axis at 110 K. The widths of the EPR lines corresponding to the transitions $M \leftrightarrow M-1$ and $-M \leftrightarrow -(M-1)$ are the same.

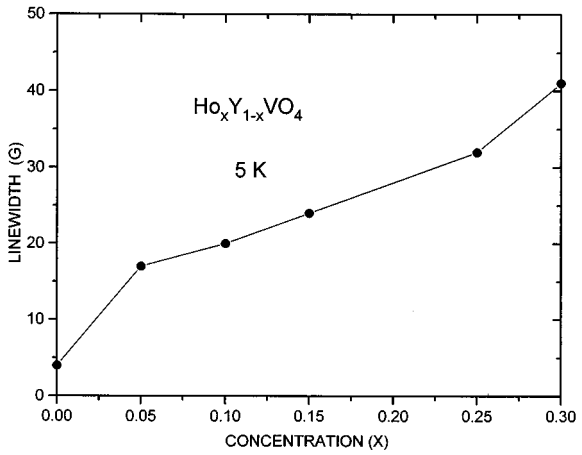


FIG. 7. Dependence of $Gd^{3+}$ EPR linewidths (G =Gauss$=10^{-4}$ T) for the central transition $(1/2\leftrightarrow -1/2)$ in $Ho_xY_{1-x}VO_4$ on concentration ($x$) of the host paramagnetic ions $Ho^{3+}$ for $\mathbf{B}\|Z$ axis at 5 K.

According to Eq. (3), the ratios of the linewidths of the various transitions relative to the outermost lines are $\Delta B(+\frac{1}{2}\leftrightarrow -\frac{1}{2})/\Delta B(\pm\frac{7}{2}\leftrightarrow\pm\frac{5}{2})=2.38$, $\Delta B(\pm\frac{1}{2}\leftrightarrow\pm\frac{3}{2})/\Delta B(\pm\frac{7}{2}\leftrightarrow\pm\frac{5}{2})=2.23$, $\Delta B(\pm\frac{3}{2}\leftrightarrow\pm\frac{5}{2})/\Delta B(\pm\frac{7}{2}\leftrightarrow\pm\frac{5}{2})=1.77$. Thus, the outer resonance lines become progressively narrower due to ''lifetime broadening'' with respect to the central line. As seen from Figs. 3 and 4, the observed linewidths are in fact not in accordance with the ratios predicted by ''lifetime broadening,'' since, as discussed below, there exist other sources of the broadening such as disorder in $Tm_xLu_{1-x}PO_4$ samples, and inhomogeneous broadening due to superhyperfine (SHF) interactions in $Ho_xY_{1-x}VO_4$. The unique features of the behavior of $Gd^{3+}$ EPR linewidths specific to the two families of crystals, are described as follows.

### $Ho_xY_{1-x}VO_4$ samples

*Dependence on concentration* ($x$) *and formation of percolation clusters*. For the crystals with smaller concentrations $x=0.1$–$0.25$, only a weak dependence of the EPR linewidths on $x$ was observed. For $Ho_{0.3}Y_{0.7}VO_4$ sample, there was observed a sharp increase of the EPR linewidths as compared to those for $x\leqslant 0.25$, in the range 77–300 K. This can be explained to be due to the formation of a percolation cluster within the crystal for $x>0.25$, which shortens significantly the relaxation times of the $Gd^{3+}$ ions by spin diffusion as discussed in detail by Misra and Orhun[17] in context with $LiYb_xY_{1-x}F_4$ crystals. When the relaxation time is shortened it manifests in an increase in EPR linewidth. As for the formation of percolation clusters, the calculations of the $LiYb_xY_{1-x}F_4$ system can be adopted directly for the $Ho_xY_{1-x}VO_4$ samples, since the scheelite structure of $LiYbF_4$ is similar to that of the zircon structure of $HoVO_4$, in which there are situated four nearest ($R_N=3.893$ Å), and four next-nearest ($R_{NN}=5.910$ Å) and eight next-next-nearest ($R_{NNN}=5.938$ Å) neighbor rare-earth ions around any rare-earth ion. In the percolation-cluster computations for $LiYbF_4$ only the nearest ($R_N=5.13$ Å, four ions) and next-nearest ($R_{NN}=5.88$ Å, four ions) neighbors were considered. The critical value of $x$ was found to be 0.27, above which a percolation cluster was formed extending throughout the entire sample. Since the critical value of $x$ in percolation-cluster calculations depends only on geometrical configuration of the rare-earth ions surrounding the $Gd^{3+}$ ion, rather than on the absolute distance between the rare-earth ions, the percolation-cluster consideration for $LiYb_xY_{1-x}F_4$ for zircon structure limited up to four nearest-neighbor ions is directly applicable to $Ho_xY_{1-x}VO_4$ crystals. Thus, ignoring the small configurational difference between the arrangement of the rare-earth ions in zircon and scheelite structures, the critical value $x\approx 0.27$ is also expected for $Ho_xY_{1-x}VO_4$ samples.

*Temperature dependence*. The $Gd^{3+}$ EPR linewidths in $Ho_xY_{1-x}VO_4$ samples with $0.1<x<0.3$ were observed to vary insignificantly in the 150–300 K range. It was only below 150 K that the $Gd^{3+}$ EPR linewidth for these samples increased significantly with decreasing temperature as seen from Fig. 4; very broad EPR lines were observed in particular in $Ho_{0.3}Y_{0.7}VO_4$ sample. However, at liquid-helium temperatures $Gd^{3+}$ EPR linewidth decreased, and well-resolved EPR $Gd^{3+}$ spectra were observed characterized by rather narrow lines as the effective $Ho^{3+}$ magnetic moment became negligible due to preferential population of the nonmagnetic singlet ground state, as seen from Fig. 2 for $Ho_{0.3}Y_{0.7}VO_4$ at 5 K. As for the more concentrated $Ho_xY_{1-x}VO_4$ samples with $x>0.3$, *no* EPR spectra could be observed in the interval 77–300 K due to EPR lines being completely broadened out, presumably due to formation of percolation clusters.

#### Liquid-helium temperatures ($x=0.05$, 0.1, 0.15, 0.25, 0.3)

$Gd^{3+}$ EPR spectrum could only be observed for the orientations of **B** near and parallel to the $Z$ axis in $Ho_xY_{1-x}VO_4$ samples with $0.05\leqslant x\leqslant 0.3$; the linewidth increased with increasing deviation of the magnetic-field orientation from the magnetic $Z$ axis, disappearing completely for **B** orientation at angles larger than about 30°–50° from the $Z$ axis in the $ZX$ plane. This disappearance of EPR spectrum at low temperatures, when the angle between the orientation of the external magnetic field and $Z$ axis increases, can be explained to be due to the large anisotropy of magnetic moment of the $Ho^{3+}$ ions in $HoVO_4$, resulting in $\langle M_\perp\rangle\gg\langle M_z\rangle$.[28]

In $Ho_{0.3}Y_{0.7}VO_4$ sample, the presence of at least three different sets of $Gd^{3+}$ EPR spectra could be discerned at liquid-helium temperature (Fig. 2), characterized by different linewidth and temperature behaviors. This can be explained to be due to the rather significant interaction of the electronic quadrupole moments of $Ho^{3+}$ ions with the neighbor atoms on the lattice of $Ho_xY_{1-x}VO_4$ samples at temperatures below 100 K, which arises due to highly aspherical ground-state $4f$ charge distribution as reported by Skanthakumar *et al.*,[21] observing large magnetic anisotropy at low temperatures. The asphericity is a consequence of electronic quadrupole moment to first order. Decrease in temperature from room temperature increases the asphericity as the excited energy levels become more and more depopulated in favor of the ground singlet state characterized by a highly anisotropic configuration. Specifically, this means that although the unit-cell parameters of $HoVO_4$ and $YVO_4$ are very close to each

other at room temperature, they become anomalously different from each other below 100 K as the parameters of the $HoVO_4$ lattice change significantly due to the interaction of $Ho^{3+}$ electronic quadrupole moment with the neighbor atoms on the lattice. In addition to the effect of $Ho^{3+}$ ionic quadrupole moment, the presence of $Ho^{3+}$ ions in the vicinity of a $Gd^{3+}$ ion, characterized by different relative directions of the external magnetic field with respect to the vectors joining different $Ho^{3+}$ ions with the $Gd^{3+}$ ion result in a large variety of magnetically different configurations that increase the linewidths and modify line positions. It is difficult to predict uniquely which specific configurations result around $Gd^{3+}$ ions for different concentrations ($x$) of $Ho^{3+}$ ions. The particular features of the values of the spin-Hamiltonian parameters corresponding to distinct observed sets of $Gd^{3+}$ spectra can be described as follows. (The values of the parameters have been listed in Sec. IV above.) The maximum magnitude of $b_2^0$ characterizing the various observed spectra is very close to that of the $Gd^{3+}$ ion in $YVO_4$. On the other hand, the magnitude of the parameter $b_2^0$ for $HoVO_4$ [$=-1.083$ GHz (Ref. 10)] is much less than this. This implies that of the three observed spectra those characterized by the maximum, next maximum, and minimum magnitudes of $b_2^0$ correspond to the $Gd^{3+}$ environment with zero, one, and two $Ho^{3+}$ ions, respectively, as the nearest neighbors. For the spectrum characterized by the maximum magnitude of $b_2^0$, the linewidths of all the transitions are the same, being 39 G at 5 K and 42 G at 10 K. For the spectrum with the second largest value of $b_2^0$ at 5 K, the central line (40 G) is narrower than the outer lines (52 and 90 G for the transitions $\pm 3/2 \leftrightarrow \pm 1/2$ and $\pm 5/2 \leftrightarrow \pm 3/2$, respectively) indicating the presence of disorder created by the four different possible configurations of the presence of one $Ho^{3+}$ ion nearest to a $Gd^{3+}$ ion. There exist six different possible configurations for the case of two $Ho^{3+}$ ions being nearest neighbors to a $Gd^{3+}$ ion, causing more disorder than that expected for the case of one $Ho^{3+}$ ion as the nearest neighbor. However, it was difficult to discern the linewidths from the observed spectra for this configuration as the corresponding EPR lines were rather weak and superimposed by other lines. As for the temperature dependence of the EPR linewidth, it is noted that the more $Ho^{3+}$ ions are next neighbors to a $Gd^{3+}$ ion, the stronger the temperature dependence is expected to be due to dipole-dipole and exchange interactions between $Gd^{3+}$ and $Ho^{3+}$ ions, consequently the spectrum is expected to disappear faster with increasing temperature as the $Ho^{3+}$ magnetic moment increases with temperature. Accordingly, in the $Ho_{0.3}Y_{0.7}VO_4$ sample, the EPR spectra of $Gd^{3+}$ ion possessing the largest, second largest, and minimum magnitudes of $b_2^0$ disappeared at about 10, 7, and 5 K, respectively, as the temperature was increased.

In $Ho_{0.25}Y_{0.75}VO_4$ and $Ho_{0.15}Y_{0.85}VO_4$ samples, only two distinct sets of overlapping $Gd^{3+}$ EPR spectra were observed, the value of the parameter $b_2^0$ (Sec. IV) of the more intense $Gd^{3+}$ EPR spectrum being the same as that for $Gd^{3+}$ in $YVO_4$.[7] The main EPR spectrum disappeared at about 22–25 K as the temperature increased. The linewidths did not practically change in this temperature range. One set of $Gd^{3+}$ EPR spectrum was much weaker than the other spectrum, the value of the parameter $b_2^0$ characterizing this spectrum being the same as that for the $Gd^{3+}$ EPR spectrum with the second largest $b_2^0$ magnitude in $Ho_{0.3}Y_{0.7}VO_4$ (listed in Sec. IV). This weaker $Gd^{3+}$ EPR spectrum disappeared at about 10 and 5 K in $Ho_{0.25}Y_{0.75}VO_4$ and $Ho_{0.15}Y_{0.85}VO_4$, respectively, as the temperature was increased. In $Ho_{0.1}Y_{0.9}VO_4$ only one$Gd^{3+}$ EPR spectrum was observed, which disappeared at about 25 K. In $Ho_{0.25}Y_{0.75}VO_4$, $Ho_{0.15}Y_{0.85}VO_4$, and $Ho_{0.1}Y_{0.9}VO_4$ the predominant $Gd^{3+}$ EPR spectra are those due to the $Gd^{3+}$ ion surrounded only by $Y^{3+}$ ions, since the magnitudes of the parameter $b_2^0$ characterizing these spectra are practically the same as that for $YVO_4$. For all $Ho_xY_{1-x}VO_4$ samples at liquid-helium temperatures the linewidths are the same for all transitions within experimental error ($\pm 1$ G).

*Temperature dependence of the magnetic moment of $Ho^{3+}$ ions and its effect on the linewidth*. A calculation was made of the temperature dependence of the $Z$ component of the average magnetic moment, $\langle M_z \rangle$, of the host $Ho^{3+}$ ion, using the expression

$$\langle M_z \rangle = \sum_i \langle \varphi_i | J_z | \varphi_i \rangle \exp(-E_i/kT) / \sum_i \exp(-E_i/kT). \tag{4}$$

In Eq. (4), $|\varphi_i\rangle$, $E_i$ are the eigenvectors and eigenvalues of the crystal-field Hamiltonian for $Ho^{3+}$ ions: $H_{\mathrm{CEF}}|\varphi_i\rangle = E_i|\varphi_i\rangle$, where $H_{\mathrm{CEF}}$ is expressed as follows:

$$H_{\mathrm{CEF}} = \mu_B g_J B_z J_z + \alpha_2 B_2^0 O_2^0 + \alpha_4 (B_4^0 O_4^0 + B_4^4 O_4^4) + \alpha_6 (B_6^0 O_6^0 + B_6^4 O_6^4). \tag{5}$$

In Eq. (5), $g_J = 1.2417$,[24] $J(=8)$ is the angular momentum of the $Ho^{3+}$ ion, the spin operators $O_n^m$ for $J=8$ are defined and listed by Abragam and Bleaney.[24] The following CEF parameters were used in Eq. (5) in the calculations: $B_2^0 = -87.6\ \mathrm{cm}^{-1}$, $B_4^0 = 38.2\ \mathrm{cm}^{-1}$, $B_4^4 = -768\ \mathrm{cm}^{-1}$, $B_6^0 = -43.1\ \mathrm{cm}^{-1}$, $B_6^4 = 77.8\ \mathrm{cm}^{-1}$, as estimated by Morin, Rouchy, and Kazei.[27] The resulting temperature variation of $\langle M_z \rangle$ is plotted in Fig. 8, which shows that $\langle M_z \rangle$ increases with decreasing temperature and decreases very sharply at liquid-helium temperatures. It can be explained to be due to the profound effect of the first-excited doublet, with the energy 21 $\mathrm{cm}^{-1}$, whose eigenvectors are predominantly $|M_J = \pm 1\rangle$, where $M_J$ is the magnetic quantum number corresponding to $J_z$ of the $Ho^{3+}$ ion, as well as that of the second excited doublet of the $Ho^{3+}$ ion with the energy 47 $\mathrm{cm}^{-1}$ whose eigenvectors are predominantly $|M_J = \pm 7\rangle$,[27] possessing a rather large value of $\langle M_z \rangle$. This temperature behavior is similar to that of the observed $Gd^{3+}$ EPR linewidth in $Ho_xY_{1-x}VO_4$ ($0.1 \leqslant x \leqslant 0.3$) crystals. Thus, it can be concluded that the temperature variation of the $Gd^{3+}$ EPR linewidth in $Ho_xY_{1-x}VO_4$ crystals in the temperature range 4–300 K is significantly determined by the temperature variation of the magnetic moments of the surrounding host $Ho^{3+}$ ions situated in close proximity with the $Gd^{3+}$ ions, because of their interaction with the latter.

*Disorder*. Unlike that for $Tm_xLu_{1-x}PO_4$ crystals (discussed below), disorder is practically absent in

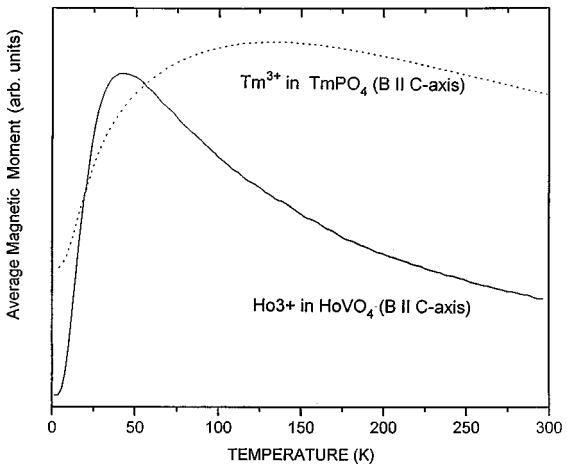


FIG. 8. Calculated temperature dependences of the average magnetic moment, $\langle M_z \rangle$, of host paramagnetic ions $Tm^{3+}$ (dotted line) and $Ho^{3+}$ (continuous line) in $Tm_xLu_{1-x}PO_4$ and $Ho_xY_{1-x}VO_4$ compounds, respectively, for $\mathbf{B} \| c$ axis.

$Ho_xY_{1-x}VO_4$ samples at all temperatures because (i) the ionic radii of the $Ho^{3+}$ and $Y^{3+}$ ions are almost about the same, being 0.894 and 0.893 Å, respectively,[29] and (ii) the unit-cell parameters of the two constituting lattices: $a=b=7.1237$ Å, $c=6.2890$ Å for $HoVO_4$ and $a=b=7.1193$ Å, $c=6.2892$ Å for $YVO_4$ (Ref. 23) are almost the same.

*Broadening due to superhyperfine (SHF) interactions.* In $Ho_xY_{1-x}VO_4$ samples with $x=0.1$, 0.15, 0.25, and 0.3, the central $Gd^{3+}$ line was broader than the outer lines in the temperature range 77–300 K, similar to that expected when ''lifetime broadening'' is effective. However, this is not entirely due to lifetime broadening, since the ratios of the widths of different transition lines are far from those predicted by Mehran and Stevens[12] for ''lifetime broadening.'' The observed broadening of the central line over and above that expected from ''lifetime broadening'' can be explained to be due to the presence of a rather large background EPR linewidth, ascribed mainly to indirect SHF interaction between the $Gd^{3+}$ ion and $^{165}Ho$ nuclei (magnetic moment $=0.466$ nm),[10] which is temperature independent and is the same for all transitions. The linewidth due to SHF interaction in $Ho_xY_{1-x}VO_4$ crystals can be considered to be mainly that observed at liquid-helium temperatures, where the effect of ''lifetime broadening'' is expected to be negligible because the host $Ho^{3+}$ ions are in the singlet nonmagnetic ground state. As the concentration ($x$) increases, there is expected an increase in the linewidth due to SHF interaction because of increasing number of $^{165}Ho$ nuclei in the neighborhood of a $Gd^{3+}$ ion. This is clearly seen from Fig. 7, which exhibits the dependence of the EPR linewidth on concentration ($x$) at 5 K.

*Lifetime broadening.* In $Ho_{0.02}Y_{0.98}VO_4$ and $Ho_{0.05}Y_{0.95}VO_4$ samples, there is not expected any significant ''background'' EPR linewidth due to SHF interactions, because of the negligible number of $Ho^{3+}$ ions present in these samples. However, for samples with higher concentrations $x$ (0.1, 0.15, 0.25, 0.3) there do exist some residual EPR linewidths, estimated to be 15 G for the samples $Ho_{0.1}Y_{0.9}VO_4$, $Ho_{0.15}Y_{0.85}VO_4$, and $Ho_{0.25}Y_{0.75}VO_4$ at 78 K and 40 G for $Ho_{0.3}Y_{0.7}VO_4$ at 110 K, so that after subtracting these from the observed linewidths the ratios conform to those expected for ''lifetime broadening'' (see Table III).

### $Tm_xLu_{1-x}PO_4$ samples

*Temperature and concentration dependence.* The $Gd^{3+}$ EPR spectra could be observed at all temperatures for all

TABLE III. Estimated ratios of the $Gd^{3+}$ EPR linewidths due to magnetic interactions with the host paramagnetic ions $\Delta B_i' = (\Delta B_i - \Delta B_0)$; $i=1,2,3,4$, of the various transitions at liquid-nitrogen temperature due to exchange and dipole interactions for $Ho_xY_{1-x}VO_4$ ($x=0.1$, 0.15, 0.25, 0.3) and $Tm_{0.8}Lu_{2.0}PO_4$, $\mathbf{B} \| Z$ axis. (Here $\Delta B_1$, $\Delta B_2$, $\Delta B_3$, $\Delta B_4$ represent, respectively, the observed widths of the lines corresponding to the transitions $\pm 7/2 \leftrightarrow \pm 5/2$, $\pm 5/2 \leftrightarrow \pm 3/2$, $\pm 3/2 \leftrightarrow \pm 1/2$, $+1/2 \leftrightarrow -1/2$, while $\Delta B_0$ represents the ''background'' EPR linewidth, namely, the part which is not due to the exchange and dipolar interactions as discussed in Sec. V.) For $Ho_xY_{1-x}VO_4$, $\Delta B_0$ is considered to be due to the SHF interaction of $Gd^{3+}$ with the nearest- and next-nearest $^{165}Ho$ nuclei; it has the same value for all the transitions. For $Tm_{0.8}Lu_{0.2}PO_4$, $\Delta B_0$ is considered to be due mainly to disorder, $\Delta B_i$ are assumed to be equal to the respective widths of the various transitions observed at the lowest temperature (5 K): $\Delta B_4=25$ G, $\Delta B_3=37$ G, $\Delta B_2=44$ G, $\Delta B_1=68$ G. For both families of host crystals, no influence of exchange and dipolar interactions of the $Gd^{3+}$ ion with the host paramagnetic ions is expected at 5 K as both the $Ho^{3+}$ and $Tm^{3+}$ ions are in their respective nonmagnetic singlet ground states.

| | $\Delta B_0$ (G) | $T$ (K) | $\Delta B_4'/\Delta B_1'$ | $\Delta B_3'/\Delta B_1'$ | $\Delta B_2'/\Delta B_1'$ |
|---|---|---|---|---|---|
| Lifetime Broadening (Ref. 12) | | | 2.38 | 2.23 | 1.77 |
| $Ho_{0.1}Y_{0.9}VO_4$ | 15 | 78 | 2.3 | 2.0 | 1.6 |
| $Ho_{0.15}Y_{0.85}VO_4$ | 15 | 78 | 2.3 | 2.1 | 1.8 |
| $Ho_{0.25}Y_{0.75}VO_4$ | 16 | 78 | 2.4 | 2.1 | 1.8 |
| $Ho_{0.3}Y_{0.7}VO_4$ | 40 | 110 | [a] | 2.1 | 1.7 |
| $Tm_{0.8}Y_{0.2}PO_4$ | [b] | 78 | 2.34 | 2.1 | 1.74 |

[a]Corresponding EPR line is not resolved.
[b]Listed in the caption.

concentrations ($x$) of $Tm^{3+}$ ions in this family of crystals. No temperature dependence of the EPR linewidth of samples with $x=0.1$, 0.2, 0.4, 0.6 was observed in the interval 77–300 K. The outer EPR lines for these samples were observed to be significantly wider relative to the central line. The behavior of $Gd^{3+}$ EPR linewidths for the samples with $x=0.4$ and 0.6, more concentrated in $Tm^{3+}$ ions was different from this, in that the outer lines here are only slightly broader than the central one. This is due to lifetime broadening.[9]

*Effect of magnetic moment of $Tm^{3+}$ ions*. A calculation of the average magnetic moment $\langle M_z \rangle$ of the $Tm^{3+}$ ($J=6$) ion was made as a function of temperature using Eq. (4), and the CEF Hamiltonian given by Eq. (5) with the values of the parameters: $g_J=1.1638$, $B_2^0=132$ cm$^{-1}$, $B_4^0=4.1$ cm$^{-1}$, $B_4^4=642$ cm$^{-1}$, $B_6^0=44$ cm$^{-1}$, $B_6^4=-10.9$ cm$^{-1}$ as determined by Hodges.[30] The resulting values are plotted in Fig. 8, which shows that as the temperature is decreased from 300 K, $\langle M_z \rangle$ remains almost constant down to 150 K, below which it decreases with decreasing temperature, in the same fashion as the $Gd^{3+}$ EPR linewidth for $\mathbf{B} \| Z$ axis, shown in Fig. 3. Thus, in $Tm_xLu_{1-x}PO_4$ samples, similar to that in $Ho_xY_{1-x}VO_4$ samples, the average magnetic moment of the host $Tm^{3+}$ ions determines predominantly the temperature variation of the $Gd^{3+}$ EPR linewidth.

*Effect of disorder*. The broadening of EPR lines for $Tm_{0.1}Lu_{0.9}PO_4$ and $Tm_{0.2}Lu_{0.8}PO_4$ samples, and appearance of additional sets of $Gd^{3+}$ EPR spectra with different linewidths observed at liquid-nitrogen temperature [Fig. 1(a)] which overlap the main set of lines can be ascribed to the disorder in the atomic arrangement in these mixed crystals. Disorder broadens outer-lying EPR transition lines relative to the central line, the width increasing almost linearly with the separation of an outer line position from that of the central line.[24] The disorder in $Tm_xLu_{1-x}PO_4$ compounds is caused by both the difference in the ionic radii of the $Tm^{3+}$ and $Lu^{3+}$ ions, being 0.85 and 0.87 Å,[29] respectively, and the differences in the unit-cell parameters of the pure paramagnetic lattices: $a=b=6.8424$ Å and $c=5.9895$ Å for $TmPO_4$ and for the pure diamagnetic lattice $LuPO_4$ at room temperature: $a=b=6.7937$ Å and $c=5.9582$ Å.[23] Disorder causes increase in the splitting of EPR lines with increasing concentration ($x$). For example, in the $Tm_{0.2}Lu_{0.8}PO_4$ sample there are clearly observed two sets of $Gd^{3+}$ lines at 77 K due to the existence of at least two magnetically inequivalent $Gd^{3+}$ sites characterized by different linewidths, resulting in two overlapping lines for the highest-field transition, one with the width 37 G, and other with the width 70 G. This is because of the various theoretically possible configurations, one $Gd^{3+}$ site has all the nearest ions to be (diamagnetic) $Lu^{3+}$ ions, while the other site has at least one (paramagnetic) $Tm^{3+}$ ion as the nearest neighbors. The effect of the electronic quadrupole moment of the $Tm^{3+}$ ion on the local structure of $Tm_xLu_{1-x}PO_4$ appears to be negligible, unlike that in $Ho_xY_{1-x}VO_4$ samples.

*Lifetime broadening*. Only for the $Tm_{0.8}Lu_{0.2}PO_4$ sample was there observed a significant influence of dipole-dipole and exchange interactions, as here the outer lines were observed to be narrower relative to the central line, unlike that for the samples with smaller concentrations of $Tm^{3+}$ ions ($x<0.8$). However, even in this sample disorder is significant, because at 5 K the central line is observed to be narrower than the outer lines as expected from disorder, while the host $Tm^{3+}$ ions are in the nonmagnetic singlet ground state not to have any magnetic interaction with the $Gd^{3+}$ ion. Influence of SHF interaction with $Tm^{3+}$ ions was also observed on the $Gd^{3+}$ linewidth in this sample, because the width (25 G) of the central line is the same as that in the pure $TmPO_4$ sample,[13] and much larger than that observed in the purely diamagnetic $LuPO_4$ sample (3.5 G). For the $Tm_{0.8}Lu_{0.2}PO_4$ sample, when the observed widths of the EPR lines at 5 K are subtracted off from the widths of the respective EPR lines at liquid-nitrogen temperatures, the relations between the EPR linewidth of different transitions are found to be the same as those expected for lifetime broadening[12] as seen from Table III. There appears some temperature dependence of the EPR linewidth in $Tm_{0.6}Lu_{0.4}PO_4$ sample in the temperature range 4.2–110 K, presumably due to the temperature variation of the magnetic moment of the $Tm^{3+}$ ion.

*Percolation clusters*. The formation of percolation clusters for $Tm_xLu_{1-x}PO_4$ samples with $x>0.3$ is not well defined, unlike that in the case of $Ho_xY_{1-x}VO_4$ crystals, for the following reasons: (i) Dipole-dipole and exchange interactions of the $Gd^{3+}$ ion with the host paramagnetic ions are not as strong in $Tm_xLu_{1-x}PO_4$ as those in $Ho_xY_{1-x}VO_4$ as revealed by the EPR linewidth behavior; specifically in $TmPO_4$, EPR lines can be observed over the entire 4.2–300 K range,[8] while in $HoVO_4$ the EPR lines are observed only below 10 K.[10] (ii) The disorder that occurs in $Tm_xLu_{1-x}PO_4$ samples prevents formation of percolation clusters by disrupting percolation paths, unlike that in $HoVO_4$ samples.

*SHF interactions*. Although the nuclear magnetic moments of $^{169}$Tm (1.192 nm) is much larger than that of $^{165}$Ho (0.466 nm), the effect of SHF interaction between $Gd^{3+}$ ions and $^{169}$Tm nuclei is not expected to be significant, because the nuclear spin ($I=1/2$) of the $^{169}$Tm nucleus is much smaller than that of the $^{165}$Ho nucleus ($I=7/2$). Thus, unresolved $Gd^{3+}$ EPR lines for $TmPO_4$ consist of only five components due to the four-nearest $Tm^{3+}$ ions, much fewer than the 29 SHF components expected due to the four nearest $Ho^{3+}$ ions in $HoVO_4$.

## VI. SPECTRUM OF $Er^{3+}$ IN $Ho_xY_{1-x}VO_4$ ($x=0.1$, 0.15, 0.25, 0.3)

The samples contained $Er^{3+}$ ions as chemical impurity. The EPR line of the $Er^{3+}$ ion in $Ho_{0.3}Y_{0.7}VO_4$ sample was observed in the temperature range 4.2–10 K. At temperatures below 5 K, it was an overlap of at least two single $Er^{3+}$ EPR lines with different linewidths (43 and 134 G), possessing the same value of $g_\parallel$ ($=3.559$). In $Ho_{0.25}Y_{0.75}VO_4$, $Ho_{0.15}Y_{0.85}VO_4$, $Ho_{0.1}Y_{0.9}VO_4$, and $Ho_{0.05}Y_{0.95}VO_4$ samples, $Er^{3+}$ EPR spectra were also observed in the same temperature range (4.2–25 K), the same over which the main $Gd^{3+}$ EPR spectra could be observed. This implies that the main source of broadening of EPR lines for both $Er^{3+}$ and $Gd^{3+}$ ions is the interactions with the host $Ho^{3+}$ ions. The width of the $Er^{3+}$ EPR line in these samples were about 17, 20, 25, and 33 G for $Ho_{0.05}Y_{0.95}VO_4$,

$Ho_{0.1}Y_{0.9}VO_4$, $Ho_{0.15}Y_{0.85}VO_4$, and $Ho_{0.25}Y_{0.75}VO_4$, respectively.

## VII. DISTORTION OF CRYSTAL STRUCTURE WITH CONCENTRATION ($x$)

Because of the difference in the unit-cell parameters of $HoVO_4$ and $YVO_4$, and those of $LuPO_4$ and $TmPO_4$, the distortion of the crystal structures of $Ho_xY_{1-x}VO_4$ and $Tm_xLu_{1-x}PO_4$ samples is expected to be maximum for the value of $x$ near 0.5, while no distortion is expected for $x=0.0$ and 1.0. At liquid-helium temperature ($\sim$4 K), due to magnetic moment of the host ions being almost zero, all ions being in the nonmagnetic singlet ground state, the effect of the magnetic moment of the host ions on linewidth is expected to be negligible, and the variation of the linewidth with $x$ is determined solely by distortion, e.g., in $Tm_xLu_{1-x}PO_4$ hosts at 4 K the linewidths are the same for the samples with $x=0.2$ and $x=0.8$. This effect is similar to the broadening of optical spectra of $Er^{3+}$ in $Yb_xY_{1-x}F_3$ samples,[14] where a symmetric bell-like dependence on $x$ was observed for linewidths, which in that case depended only on distortion. The situation is somewhat different at higher temperatures. Figures 5 and 6 exhibit the $Gd^{3+}$ EPR linewidths in $Tm_xLu_{1-x}PO_4$ and $Ho_xY_{1-x}VO_4$ samples as functions of $x$ at 77 and 110 K, respectively. It is noted that for $Tm_xLu_{1-x}PO_4$ hosts the change in the observed linewidth behavior is not a monotonic function of $x$, which can be explained to be due to the interaction of the $Tm^{3+}$ magnetic moment with that of the $Gd^{3+}$ ion. As the number of $Tm^{3+}$ ions increases there is an additional effect on the linewidth over and above that due to disorder.

## VIII. COMPARISON OF MAGNETIC PROPERTIES OF $Ho^{3+}$ AND $Tm^{3+}$ IONS IN $Ho_xY_{1-x}VO_4$ AND $Tm_xLu_{1-x}PO_4$ LATTICES

The host Van-Vleck paramagnetic ions interact with the $Gd^{3+}$ ion via dipolar and exchange interactions. These magnetic moments depend on temperature and their energy levels which are sensitive to distortion, whose effect is maximum for $x$ being about 0.5 as discussed in the previous section. The effect is much more pronounced for $Tm_xLu_{1-x}PO_4$ crystals because of the rather marked difference in the unit-cell parameters of the constituting pure lattices $TmPO_4$ and $LuPO_4$. For this reason, formation of percolations clusters does not take place in $Tm_xLu_{1-x}PO_4$ crystals, unlike that in $Ho_xY_{1-x}VO_4$ crystals as discussed in Sec. V. The similarity of the magnetic properties of the two paramagnetic ions is confirmed by the similarity of the temperature variation of the linewidth in the purely paramagnetic host lattices $HoVO_4$ and $TmPO_4$. Temperature variation of the calculated average magnetic moments of $Ho^{3+}$ and $Tm^{3+}$ ions in $Ho_xY_{1-x}VO_4$ and $Tm_xLu_{1-x}PO_4$ lattices, respectively, for the orientation of the external magnetic field parallel to the $c$ axis are depicted in Fig. 8. It is seen that both exhibit an increase as the temperature is decreased from room temperature, passing through a peak and finally decreasing to zero as the temperature approaches zero. The peak is, however, much sharper in the case of the $Ho^{3+}$ ion as compared to that for the $Tm^{3+}$ ion.

## IX. CONCLUDING REMARKS

The salient features of the present EPR studies are as follows.

(i) Detailed experimental data on $Gd^{3+}$ EPR linewidths in $Ho_xY_{1-x}VO_4$ and $Tm_xLu_{1-x}PO_4$ lattices measured over the extended temperature interval 4.2–295 K have been presented. Although a thorough quantitative interpretation is difficult to provide at present, it is hoped that these data will prove valuable towards further theoretical attempts to understand the interactions of the $Ho^{3+}$ and $Tm^{3+}$ ions with the $Gd^{3+}$ ion in $Ho_xY_{1-x}VO_4$ and $Tm_xLu_{1-x}PO_4$ lattices, respectively.

(ii) The specific mechanisms governing the influence of concentration ($x$) of paramagnetic host ions on EPR linewidths in the $Tm_xLu_{1-x}PO_4$ and $Ho_xY_{1-x}VO_4$ samples are quite different from each other. In $Tm_xLu_{1-x}PO_4$, disorder as caused by the difference in the ionic radii of the paramagnetic $Tm^{3+}$ and diamagnetic $Lu^{3+}$ ions, as well as by the difference in lattice parameters of $TmPO_4$ and $LuPO_4$, is predominant, impeding formation of paramagnetic percolation clusters for samples with the concentration $x \geqslant 0.3$, unlike that in $Ho_xY_{1-x}VO_4$. On the other hand, the formation of percolation clusters in $Ho_xY_{1-x}VO_4$ crystals for $x \geqslant 0.3$ is predominant as confirmed by the EPR linewidth behavior, the effect of disorder being practically negligible in these samples due to the ionic radii of the $Ho^{3+}$ and $Y^{3+}$ ions, as well as the unit-cell parameters of $HoVO_4$ and $YVO_4$, being about the same.

(iii) At liquid-helium temperatures, the effect of the electronic quadrupole moment of $Ho^{3+}$ ions on the local structure of $Ho_xY_{1-x}VO_4$ results in the creation of several magnetically inequivalent sites for $Gd^{3+}$ corresponding to different numbers of $Ho^{3+}$ ions as next neighbors, which are characterized by different $Gd^{3+}$ EPR spectra associated with different values of the respective spin-Hamiltonian parameters and their temperature behaviors.

(iv) Temperature dependences of $Gd^{3+}$ EPR linewidths in $Tm_xLu_{1-x}PO_4$ and $Ho_xY_{1-x}VO_4$ are quite different from each other in the interval 77–300 K. In $Ho_xY_{1-x}VO_4$ the EPR linewidth increases with decreasing temperature for the samples with $x>0.1$. On the other hand, in $Tm_xLu_{1-x}PO_4$, EPR linewidths do not change significantly with temperature; only for $x=0.8$ does the EPR linewidth decrease with decreasing temperature in the range 4.2–300 K. The observed temperature dependences of the $Gd^{3+}$ EPR linewidths for $\mathbf{B}\|Z$ axis in the two families of hosts are similar to those of the calculated average magnetic moments, $\langle M_z \rangle$, of the respective host paramagnetic ions, implying that the host paramagnetic ions have predominant influence on $Gd^{3+}$ EPR linewidths.

## ACKNOWLEDGMENTS

Partial financial support from the National Sciences and Engineering Research Council of Canada (Grant No. OGP 0004485) is gratefully acknowledged. We are thankful to Dr. L.P. Mezentseva and Dr. T. Yu. Chemekova for fabricating the samples.

*Permanent address: Institute of Silicate Chemistry of Russian Academy of Sciences, St. Petersburg 199155, Russia.

[1] R. T. Harley and D. I. Manning, J. Phys. C **11**, L633 (1978).

[2] V. A. Ioffe, S. I. Andronenko, I. A. Bondar', L. P. Mezentseva, A. N. Bazhan, and C. Bazan, JETP Lett. **34**, 562 (1981).

[3] R. G. Clark, A. L. Allsop, N. J. Stone, and G. J. Bowden, J. Phys. C **20**, 797 (1987).

[4] A. Abragam, V. Bouffard, C. Fermon, G. Fournier, J. Gregg, J.-F. Jacquinot, and Y. Roinel, C. R. Acad. Sci. **299**, 509 (1984).

[5] H. Suzuki, N. Nambudripad, B. Bleaney, A. L. Allsop, G. J. Bowden, I. A. Campbell, and N. J. Stone, J. Phys. C **6**, 800 (1978).

[6] M. Rappaz, L. A. Boatner, and M. M. Abraham, J. Chem. Phys. **73**, 1095 (1980).

[7] J. Rosenthal, Phys. Rev. **164**, 363 (1967).

[8] F. Mehran, T. S. Plaskett, and K. W. H. Stevens, Phys. Rev. B **16**, 1 (1977).

[9] F. Mehran, K. W. H. Stevens, T. S. Plaskett, and W. J. Fitzpatrick, Phys. Rev. B **27**, 548 (1983).

[10] F. Mehran, K. W. H. Stevens, and T. S. Plaskett, Phys. Rev. B **20**, 867 (1979).

[11] F. Mehran, K. W. H. Stevens, T. S. Plaskett, and W. J. Fitzpatrick, Phys. Rev. B **25**, 1973 (1982).

[12] F. Mehran and K. W. H. Stevens, Phys. Rep. **85**, 123 (1982).

[13] R. Yu. Abdulsabirov, S. I. Andronenko, L. P. Mezentseva, I. A. Bondar', and V. A. Ioffe, Sov. Phys. Solid State **23**, 327 (1981).

[14] I. F. Gil'fanov, B. N. Kazakov, A. F. Klimachev, and A. L. Stolov, Soviet Phys. Solid State **27**, 2131 (1985).

[15] L. E. Misiak, S. K. Misra, and P. Mikolajczak, Phys. Rev. B **38**, 8673 (1988).

[16] L. E. Misiak, S. K. Misra, and U. Orhun, Phys. Status Solidi B **154**, 249 (1989). [For the behavior of $Gd^{3+}$ EPR linewidth in the mixed lattices $Yb_xY_{1-x}Cl_3.6H_2O$ and $Pr_xY_{1-x}F_3$ refer to, respectively, S. K. Misra and P. Mikolajczak, Phys. Status Solidi B **109**, 59 (1982) and S. K. Misra, W. Korczak, S. Z. Korczak, and M. Subotowicz, Solid State Commun. **76**, 1055 (1990)].

[17] S. K. Misra and U. Orhun, J. Phys. Condens. Matter. **4**, 6459 (1992).

[18] S. K. Misra and U. Orhun, Phys. Rev. B **41**, 2577 (1990).

[19] S. H. Smith and B. M. Wanklin, J. Cryst. Growth **21**, 23 (1974).

[20] H. M. Dess and S. R. Bolin, Trans. Metall. Soc. AIME **239**, 359 (1967).

[21] S. Skanthakumar, S.-K. Loong, L. Soderholm, J. M. Richardson, Jr., M. M. Abraham, and L. A. Boatner, Phys. Rev. B **51**, 5644 (1995).

[22] U. Ranon, Phys. Lett. A **28**, 228 (1968).

[23] A. T. Aldred, Acta Crystallogr. B **40**, 569 (1984).

[24] A. Abragam and B. Bleaney, *Electron Paramagnetic Resonance of Transition Ions* (Clarendon, Oxford, 1970).

[25] S. K. Misra, J. Magn. Reson. **23**, 403 (1976).

[26] F. Mehran, K. W. H. Stevens, T. S. Plaskett, and W. J. Fitzpatrick, Phys. Rev. B **22**, 2206 (1980).

[27] P. Morin, J. Rouchy, and Z. Kazei, Phys. Rev. B **51**, 15 103 (1995).

[28] S. I. Andronenko, A. N. Bazhan, V. A. Ioffe, and Yu.P. Udalov, Sov. Phys. Solid. State **27**, 379 (1985).

[29] G. B. Bokij, *Crystal Chemistry* (Nauka, Moscow, 1971) (in Russian).

[30] J. A. Hodges, J. Phys. (Paris) **44**, 833 (1983).